KSCE Journal of Civil Engineering (2019) 23(2):711-718

DOI 10.1007/s12205-018-0700-8

Structural Engineering

pISSN 1226-7988, eISSN 1976-3808
www.springer.com/12205

Seismic Behavior of Precast Concrete Shear Walls with Different Confined Boundary Elements

Zhangfeng Zhu* and Zhengxing Guo**

Received April 9, 2018/Revised 1st: July 11, 2018, 2nd: August 26, 2018/Accepted August 31, 2018/Published Online December 17, 2018

Abstract

To ensure the mechanical property of lapped spliced reinforcement and concrete confinement of boundary elements for precast concrete shears, two kinds of constraints, local constraint by additional spiral stirrups placed around each reinforcement splicing and overall constraint by lapped welding closed stirrups replacing traditional stirrups and ties, were proposed in this paper. Low-cyclic reversed loading tests were conducted on three full scale specimens, including one reference cast-in-situ specimen, one precast concrete specimen with local constraint and one precast concrete specimen with overall constraint. By comparing the aspects of strength, stiffness, ductility and energy-dissipation capacity with that of cast-in-situ specimen, it is found that local constraint and overall constraint can be considered equivalent. However, due to the over restraint by local constraint detail, the specimen with local constraint exhibited earlier yielding, poorer energy-dissipation capacity and better ductility than that with overall constraint. Coupled with the consideration of steel usage and construction simplicity, overall constraint detail should be preferred in practical engineering.

Keywords: *precast concrete, shear walls, boundary elements, concrete confinement, seismic performance*

1. Introduction

Nowadays, precast concrete structures have been rapidly developed worldwide, especially in China, due to their better quality, faster construction, less labor cost as well as less environmentally impact compared with traditional cast-in-situ concrete structures (Yee, 2001). Shear walls with adequate strength and strength have been proved to provide well protection against the collapse of whole structure as well as the damage of non-structural components in the Chile earthquake in 1985 (Wood *et al*., 1987). Thus, shear walls have been commonly used as lateral force resisting components in high-rise buildings in China. Obviously, precast concrete shear walls can take full advantages of precast concrete technology and shear walls and have become the research and application focus in China

With respect to precast concrete shear wall structure, reliable joints between precast concrete shear wall panels along the vertical and horizontal directions are the most critical aspect to ensure the structural integrity and satisfied seismic performance. Moreover, the vertical joints, which are more vital than the horizontal joints when precast concrete shear walls carry both vertical and horizontal loads, have been emphasized. There are two main categories in the design and detail of the vertical joints, which can be called as emulative and non-emulative joints. As for emulative joints, their structural performance should be equivalent to that of cast-in-place monolithic joints (ACI, 2009). Thus, emulative joints generally have the similar detail to cast-in-place joints except that the reinforcements across the joints are cut and protruded in factory for panel prefabricating and connected on site for continuity by suitable methods. Except for connection by cast-in-situ concrete (Li *et al.,* 2017; Li *et al*., 2018a, b), the most well-known rebar connection is utilizing grout-filled mechanical splice sleeves (ACI 318, 2011; Einea *et al.,* 1995; Jansson, 2008; Lu *et al*., 2017; Henin and Morcous, 2015). In China, there is another rebar connection technology widely used in precast concrete shear walls, as shown in Fig. 1. The vertical connection reinforcements across the joint are grouted in the embedded metal bellows tied to the corresponding vertical reinforcements of the reinforcement cage. Acturally, it forms a non-contact lap splice with which the force transfer between the lapped rebars occurs through the surrounding concrete. Thus, transverse reinforcements are typically required to bear splitting stress resulted from the eccenticity of spliced rebar tension (McLean and Smith, 1997).

As for shear wall itself, its flexural behavior probably governs the lateral load response in high-rise building structures and it should be properly designed and detailed to achieve ductile property like beams and columns in moment frames. In this case, the details of boundary elements at two ends of shear walls will be vital because it has an important role in the deformation capacity, ductility as well as energy dissipation capacity of shear walls (Oh *et al*., 2002). Moreover, the transverse reinforcements

*Associate Professor, College of Civil Engineering, Nanjing Tech University, Jiangsu 211816, China (Corresponding Author, E-mail: zzfking2210@163.com)
**Professor, School of Civil Engineering, Southeast University, Jiangsu 210096, China (E-mail: guozx195608@126.com)

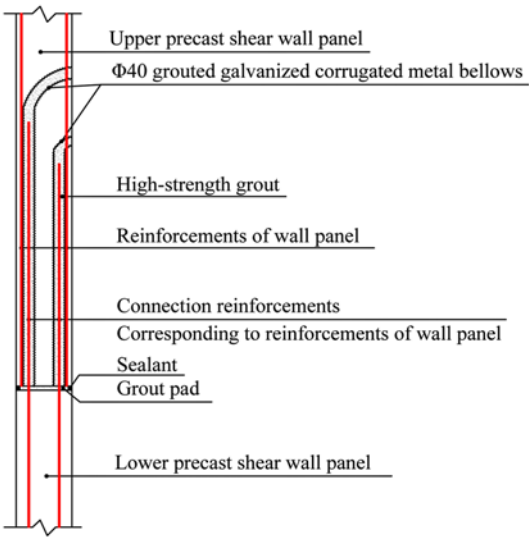

Fig. 1. Lapped Splice of Vertical Rebars

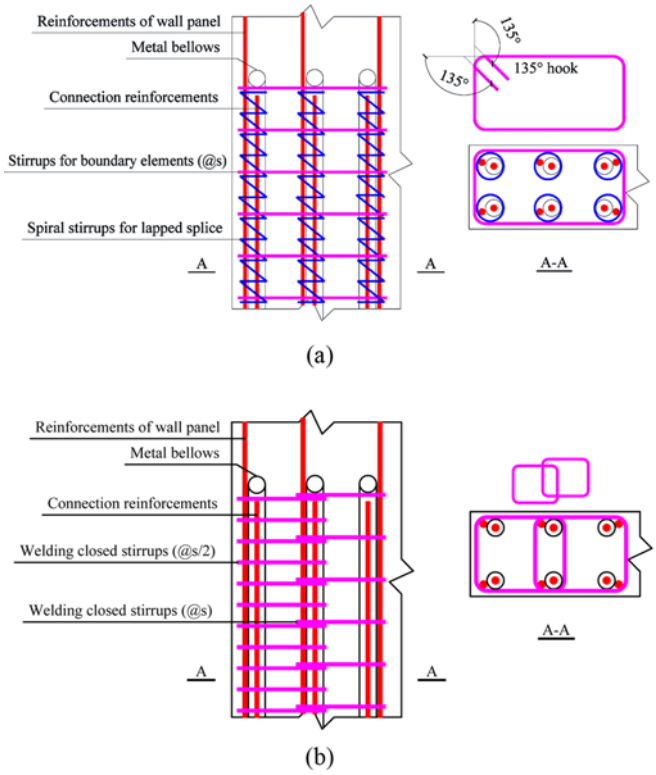

Fig. 2. Proposed Transverse Reinforcement detailing for Boundary Elements: (a) Local Constraints by Spiral Stirrups, (b) Overall Constraints by Lapped Welding Closed Stirrups

are one of the important aspects of boundary element detailing, which are aimed to confine the concrete and improve its compressive behavior under excessive inelastic deformation induced in moderate and high intensity earthquakes (Wallace and Moehle, 1992).

Hence, transverse reinforcements are quite essential in boundary elements of precast concrete shear walls for two purposes: 1) to restrain the lapped splice of rebars, and 2) to confine the concrete. Therefore, we developed two kinds of transverse reinforcement detailing to achieve the goal, as illustrated in Fig. 2. In the case of 'local constraints by spiral stirrups', traditional stirrups with 135-degree hooks at both ends are used to restrain the concrete of the boundary elements and spiral stirrups are set around the metal bellows and the vertical reinforcements to restrain the lapped splice of the rebars. In the case of 'overall constraints by lapped welding closed stirrups', traditional stirrups are replaced by welding closed stirrups. Each four vertical reinforcements are surrounded by one set of welding closed stirrups and the stirrups lapped to each other. Considering better compressive capacity required by the extreme end part of the shear wall under the combination action of the horizontal and vertical loads, the spacing of the most exterior stirrups is decreased by half to further strength the concrete constraint effect.

2. Specimen Details

Three full scale specimens, including one Cast-In-Situ Reference specimen (W-CIS), one Local Constrained Precast specimen (W-LCP) and one Overall Constrained Precast specimen (W-OCP), were made and tested to investigate the effectiveness of both local and overall constrained details. All three specimens had the same geometrical dimension and the wall panels were 200 mm in thickness, 1,700 mm in length and 3,400 mm in height. As for Specimens W-LCP and W-OCP, 20-mm thick grout pad was set on the bottom of wall panels to level and eliminate the gap between the surfaces of wall panels and foundations. Besides, topping beams with the section of 240 mm × 250 mm and foundation with dimensions of 700 mm (thickness) × 650 mm (height) × 2,300 mm (length) were also made for loading and fixing, respectively. The dimension and reinforcement detail of each specimen are shown in Fig. 3. The boundary elements at both ends were 400 mm in length, and all three specimens had the same reinforcement details except for the stirrup in boundary elements. As for Specimen W-LCP, additional spiral stirrups (Φ8@50) were placed around the rebar lapped splice, just as shown in Fig. 2(a). And Specimen W-OCP used three welding closed stirrups instead of traditional stirrups.

C35 concrete (China standard, the standard value of cubic compressive strength and the design value of compressive strength at the test day were 35 MPa and 16.7 MPa, respectively) and HRB400 (China standard, the standard the design value of

Table 1. Measured Material Strength Properties of the Specimens

Material	Compressive strength (MPa)	Yield strength (MPa)	Ultimate strength (MPa)
C35 concrete	35.9[a]	-	-
grout	75[b]	-	-
Φ8 rebar	-	452	615
Φ10 rebar	-	430	608
Φ12 rebar	-	455	602
Φ16 rebar	-	438	630

[a]The geometric size of the test coupon was 150 mm × 150 mm × 150 mm.
[b]The geometric size of the test coupon was 40 mm × 40 mm × 160 mm.

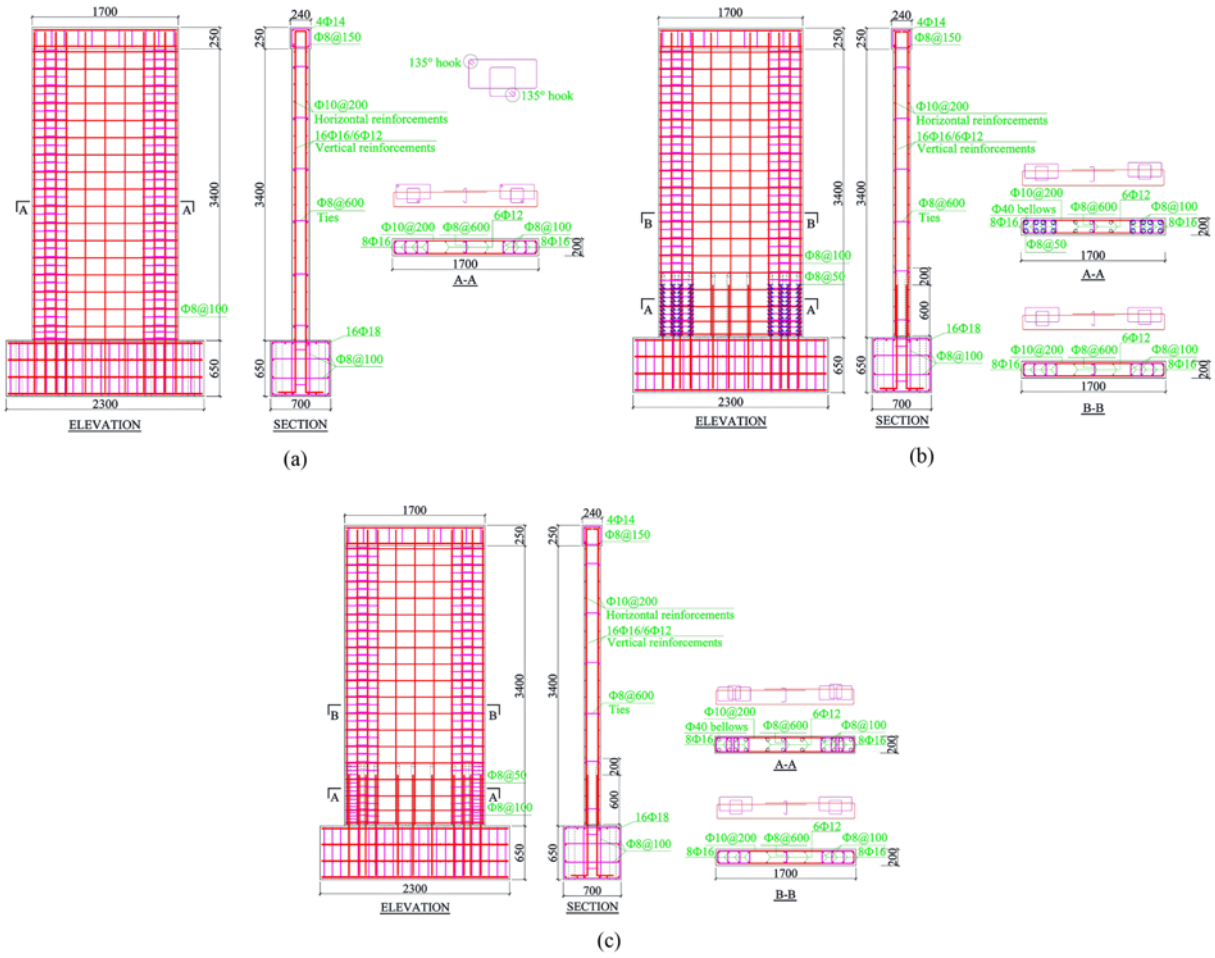

Fig. 3. Details of the Specimens: (a) W-CIS, (b) W-LCP, (c) W-OCP

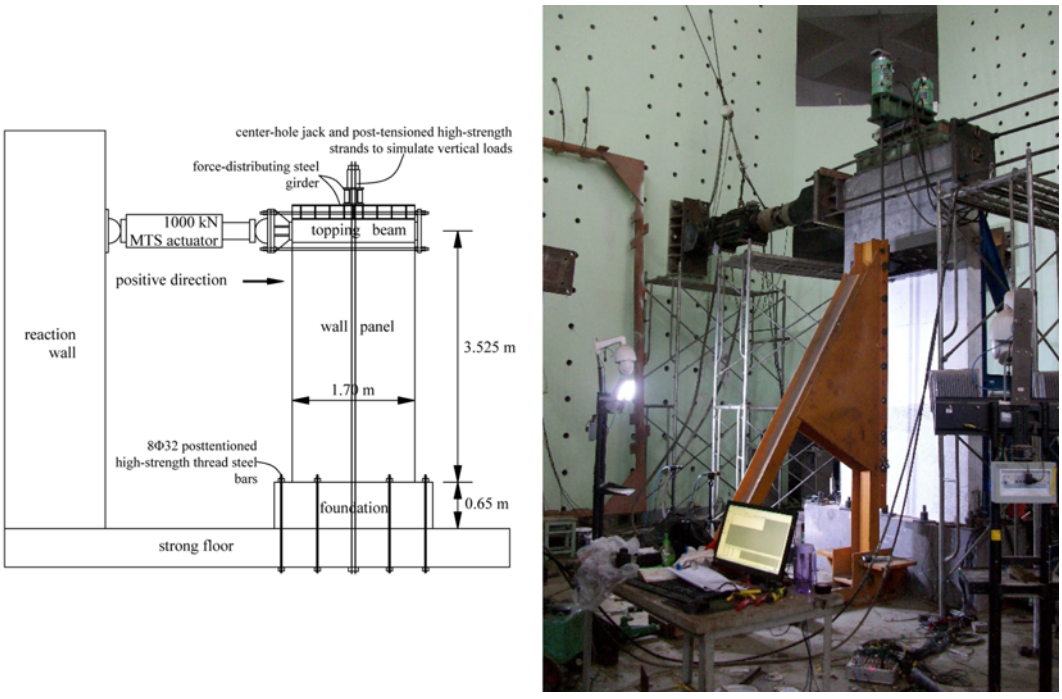

Fig. 4. Test Set-up

yield strength was 400 MPa and 360 MPa, respectively) mild steel bars were used for all specimens. The measured strengths of the concrete, the reinforcing bars and the grout are listed in Table 1.

3. Test Set-up and Procedure

Figure 4 shows the test set-up. The specimen was fixed to the strong floor of the laboratory by post-tensioned high-strength thread steel bars and were braced by two steel triangle frames as can be seen in the photo. The low-cyclic reversed lateral loading was provided by a 1,000 kN MTS actuator and was applied on the top of the specimen, acting along the axis of the topping beam. Thus, the shear-span aspect ratio of the specimen was approximately 2.1, which can be calculated as annotated in Fig. 4. A constant vertical load was applied on the specimen by post-tensioned tendons and the axial compression ratio was designed as 0.1 for each specimen.

The lateral force and deformation of the load point were measured and recorded automatically by MTS system. Strain gauges placed on the surface of the reinforcements in prior to concrete casting were used to measure strains, and Linear Variable Differential Transducers (LVDTs) were used to measure the lateral deformation of the wall panel at different heights and slippage of the foundation. The strain and deformation data were continually recorded by a data acquisition system. The vertical force was measured from oil pressure gage in the tensioning equipment for high-strength strands.

The cyclic lateral load was controlled in a manner of force and

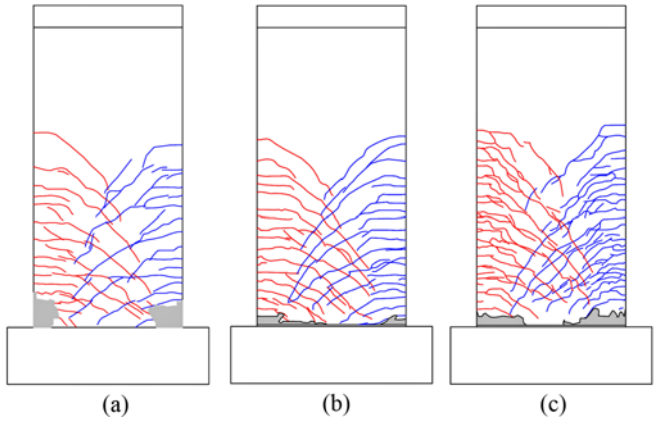

Fig. 5. Crack Patterns of the Specimens: (a) W-CIS, (b) W-LCP, (c) W-OCP

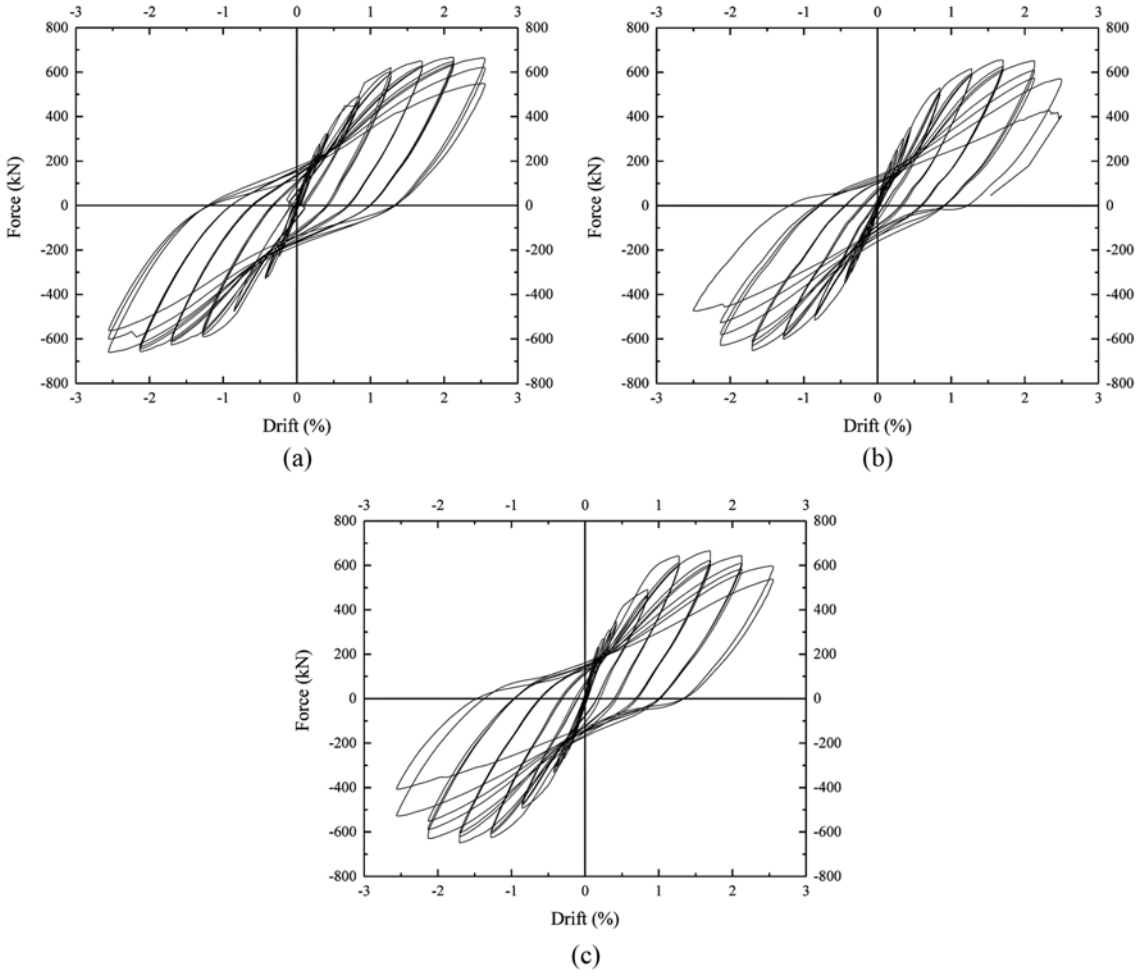

Fig. 6. Hysteretic Curves: (a) W-CIS, (b) W-LCP, (c) W-OCP

displacement. After the vertical load was applied, one-time cyclic lateral load was applied at the increasing levels of about 25−50 kN. And once the specimen entered the elastoplastic stage, three-time cyclic displacement was applied instead at the increasing levels of constant displacement. For comparable convenience, the constant displacement was determined as 15 mm, upon which the resulting drift ratio was 0.43%.

4. Measured Behavior of Specimens

4.1 Failure Modes

Initial flexural cracks occurred above the interface between wall panel and foundation under tension stress and the cracking forces were 230 kN, 200kN and 200 kN for Specimens W-CIS, W-LCP and W-OCP, respectively. As the loading force/displacement increased, new cracks occurred in the upper part of wall panel, and existing cracks extended and developed obliquely to flexure-shear cracks. The failure modes of the specimens are shown in Fig. 5, in which cracks are indicated by solid lines and hatched areas represent the crushed concrete region.

All the specimens generally behaved in flexure-shear manner and failed by fraction of longitudinal reinforcements and crushing of concrete within the boundary elements at the stage of 90-mm displacement (2.56% drift ratio) loading. Because of the discontinuity of concrete in the joint of Specimens W-LCP and W-OCP, concrete crush concentrated near the joint. The immature failure of lapped splice in Specimens W-LCP and W-OCP was avoided. It indicated that, with the help of local constraints and overall constraints, the lapped splice of the reinforcements was capable of fully developing the strength.

4.2 Hysteretic Behaviors

The measured lateral force versus lateral drift curves, representing the hysteretic behaviors of the specimens, are shown in Fig. 6. All the hysteretic loops were similar in the aspects of shape and plumpness. In the last two cycles of the same level of drift, the loading segments of the curves degrade in strength and stiffness compared with the first cycle, and the unloading segments remain almost the same as the first cycle.

4.3 Skeleton Curves

The skeleton curves of the specimens are plotted in Fig. 7. The lateral loading-carrying capacity gradually increased up to drift 1.28%, 1.70% and 1.70% for Specimens W-CIS, W-LCP and W-

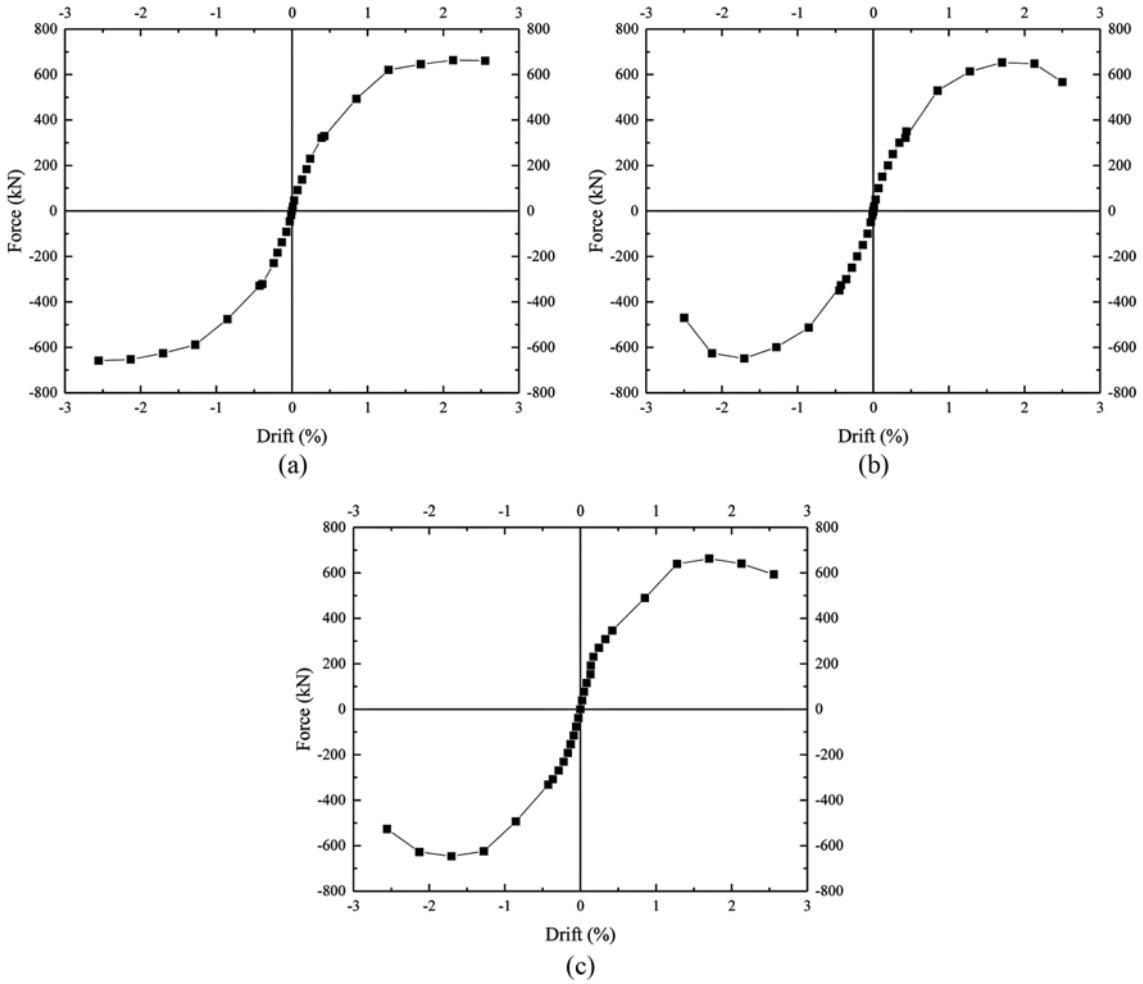

Fig. 7. Skeleton Curves: (a) W-CIS, (b) W-LCP, (c) W-OCP

OCP, respectively. Significant loss of lateral load-carrying capacity occurred in the first cycle of drift 2.56% for Specimens W-LCP and W-OCP. However, the strength of Specimen W-CIS did not happen until the third cycle of drift 2.56% (as can be seen in Fig. 6). Because of the in-plane torsion obtained in the large displacement loading stage during the experiment of Specimens W-LCP and W-OCP, the related strength and stiffness were obviously decreased. And the in-plane torsion was probably induced by the uneven and premature crush in the grout pad at the wall toes.

5. Comparison of Performance of Specimens

5.1 Strength

The strength characteristics at the stages of cracking, yielding and ultimate are listed in Table 2. The yielding strength was calculated based on reduced stiffness equivalent elasto-plastic system (Park, 1989). Due to the discontinuity of concrete across the joint, specimens W-LCP and W-OCP cracked earlier than Specimen W-CIS. Compared with Specimens W-CIS and W-OCP, Specimen W-LCP obtained the lowest yielding strength and ultimate strength. However, by comparison with Specimen W-CIS, the reduction ratios of yielding strength and ultimate strength were 4% and 2%, respectively. So, it can be concluded that the details of local and overall constraints had negligible effect on the strength of the specimens.

5.2 Stiffness

As the loading force/displacement increased, the reinforcements yield one by one, the concrete gradually damaged, and the stiffness of the specimen degraded. The stiffness of the specimen can be represented by the secant stiffness calculated based on the measured hysteretic curves. The stiffness degradation processes of the specimens are shown in Fig. 8. As indicated by the nearly coincidence curves, all the specimens possessed similar stiffness characteristics. Compared with Specimen W-CIS, the initial stiffnesses (elastic stiffnesses) of Specimens W-LCP and W-OCP were reduced by 1% and 2%, respectively. That was mainly because of the discontinuity of concrete. More obvious decrease in final stiffnesses of Specimens W-LCP and W-OCP can be found in Fig. 8. That was probably because of the in-plane torsion as mentioned above.

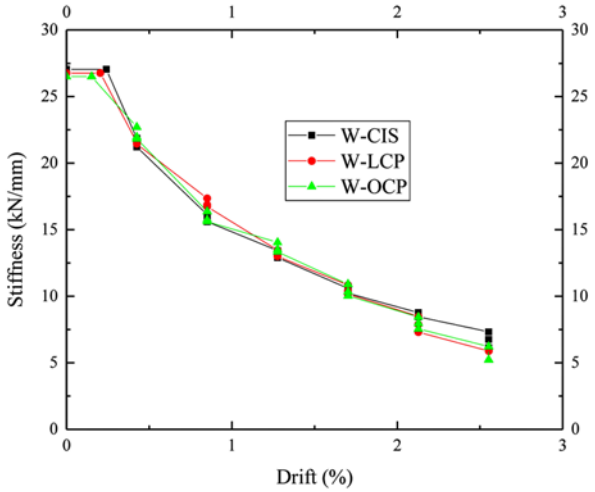

Fig. 8. Stiffness Degradation Curves of the Specimens

5.3 Ductility

Table 3 shows the displacement ductility factors of the specimens. The yielding displacement was also calculated based on reduced stiffness equivalent elasto-plastic system (Park 1989). Due to the improvement of concrete deformability resulted from both constraint details, Specimens W-LCP and W-OCP exhibited better ductility than Specimen W-CIS. Moreover, probably because of strong constraint mechanism of spiral stirrups and relatively excessive restraint, Specimen W-LCP performed better than Specimen W-OCP.

5.4 Energy-dissipation Capacity

The equivalent viscous damping ratio is utilized to assess the energy-dissipation capacity of the specimens, and the equivalent viscous damping ratios of the specimens during the stages of cracking and displacement loading are shown in Fig. 9. The energy was absorbed by means of concrete damage and reinforcing bar yielding. Thus, with the increasing of loading, the equivalent viscous damping ratio gradually increased, which can be seen in

Table 2. Cracking, Yielding and Ultimate Strengths of the Specimens

Specimen	Cracking strength (kN)			Yielding strength (kN)			Ultimate strength (kN)		
	Positive	Negative	Absolute mean	Positive	Negative	Absolute mean	Positive	Negative	Absolute mean
W-CIS	225.0	-225.0	225.0	586.8	-575.3	581.1	662.8	-658.2	660.5
W-LCP	200.0	-200.0	200.0	562.6	-555.4	559.0	653.0	-646.5	649.8
W-OCP	200.0	-200.0	200.0	597.0	-572.4	584.7	662.3	-648.6	655.5

Table 3. Displacement Ductility of the Specimens

Specimen	Yield displacement (mm)		Ultimate displacement (mm)		Displacement ductility factor (μ)		Average displacement ductility factor (μ)
	Positive	Negative	Positive	Negative	Positive	Negative	
W-CIS	41.1	-43.4	90.0	-90.1	2.19	2.08	2.14
W-LCP	36.0	-37.4	88.1	-88.1	2.45	2.36	2.41
W-OCP	40.7	-39.1	90.1	-90.1	2.21	2.30	2.26

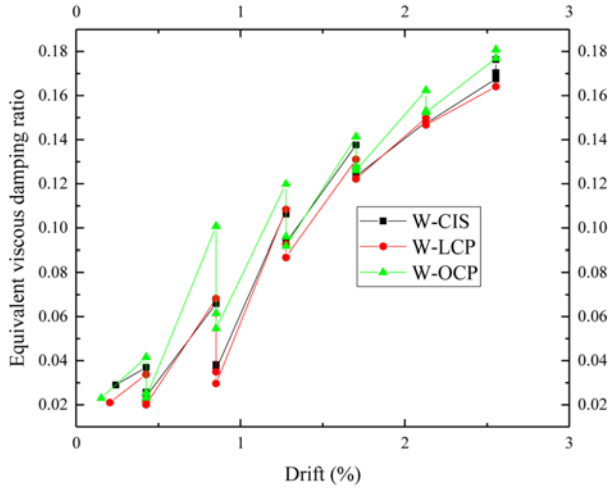

Fig. 9. Equivalent Viscous Damping Ratio of the Specimens

Fig. 9. Because the energy dissipation by the concrete damage and rebar yielding mainly occurred in the first circle, the ratios of the second and third loading cycles decreased obviously, and the curves in Fig. 9 were jagged. Moreover, Specimen W-OCP showed the best energy-dissipation capacity due to more reliable constraint by lapped closed stirrups than by traditional stirrups and more appropriate constraint than by local constraint of spiral stirrups. Besides, Specimen W-LCP possessed similar energy-dissipation capacity to Specimen W-CIS. It can be found that overall constraint detail performed better than local constraint detail and the excessively restrain brought about by local constraint reduced the concrete damage and thus weakened the energy-consumption capacity of Specimen W-LCP.

6. Conclusions

Two kinds of constrain details for the concrete within boundary elements, local constraint by spiral stirrups and overall constraint by lapped welding closed stirrups, were proposed for precast concrete shear walls. To evaluate the effect of both constraint details, pseudo-static loading tests were carried out on the corresponding specimens. Based on the test results, some conclusions were made as follows:

1. As the lapped spliced reinforcements fractured in the test, both local and overall constraints can ensure good performance of the lapped splicing of the vertical reinforcements for precast concrete shear walls.
2. The concrete within boundary elements was well confined by both local and overall constrain details. Thus, the seismic behaviors of both precast concrete specimens were similar to or even better than that of cast-in-situ specimen in terms of failure mode, hysteretic characteristic, strength, stiffness, ductility and energy-absorbing capacity.
3. Local constraint by spiral stirrups probably provided excessively restraint on the concrete within boundary elements. Thus, it caused reduced energy-dissipation capacity. However, the displacement ductility was enhanced.
4. Overall constraint by lapped welding closed stirrups well confined the boundary element concrete. Thus, the specimen with overall constraint performed best in the aspect of energy-dissipation capacity and possessed better ductility than cast-in-situ specimen.
5. In spite of the equivalent confinement effect of local constraint by spiral stirrups and overall constraint by lapped welding closed stirrups, the specimen with over constraint behaved better comprehensive performance than the specimen with local constraint. Moreover, local constraint details probably use more steels and may make reinforcement construction difficult. Thus, the detail of overall constraint will be preferred in practical engineering.

Acknowledgements

This research was funded by The National Key Research and Development Program of China (NO: 2016YFC0701703). Additional support was provided by the Nanjing Tech University; the ZHONGNAN Group, Inc.; and the Southeast University. The authors wish to acknowledge the funding agency and members participating the project for their support.

References

American Concrete Institute (ACI) (2009). *Guide to emulating cast-in-place detailing for seismic design of precast concrete structures*, ACI, Farmington Hills, MI, p. 2.

American Concrete Institute (ACI) (2011). *Building code requirements for structural concrete*, ACI, Farmington Hills, MI, p. 230.

Einea, A., Yamane, T., and Tadros, M. K. (1995). "Grout-filled pipe splices for precast concrete construction." *PCI Journal*, Vol. 40, No. 1, pp. 82-93.

Henin, E. and Morcous, G. (2015). "Non-proprietary bar splice sleeve for precast concrete construction." *Engineering Structures*, Vol. 83, pp. 154-162, DOI: 10.1016/j.engstruct.2014.10.045.

Jansson, P. O. (2008). *Evaluation of grout-filled mechanical splices for precast concrete construction*, Report No. R-1512, Michigan Department of Transportation, Lansing, MI.

Li, J., Wang, Y., Lu, Z., and Li, J. (2017). "Experimental study and numerical simulation of a laminated reinforced concrete shear wall with a vertical seam." *Applied Sciences-Basel*, Vol. 7, No. 6, p. 629, DOI: 10.3390/app7060629.

Li, J., Wang, Y., Lu, Z., and Xia, B. (2018). "Shaking table test and numerical simulation of a superimposed reinforced concrete shear wall structure." *Structural Design of Tall and Special Buildings*, Vol. 27, No. 2, p. e1412.

Li, J., Wang, L., Lu, Z., and Wang, Y. (2018). "Experimental study of L-shaped precast RC shear walls with middle cast-in-situ joint." *Structural Design of Tall and Special Buildings*, Vol. 27, No. 6, pp. e1457.

Lu, Z., Wang, Z., Li, J., and Huang, B. (2017). "Studies on seismic performance of precast concrete columns with grouted splice sleeve." *Applied Sciences-Basel*, Vol. 7, No. 6, p. 571, DOI:10.3390/app7060571.

McLean, D. I. and Smith, C. L. (1997). *Noncontact lap splices in bridge column-shaft connections*, Report No. WA-RD 417.1, Washington

State Department of Transportation, Pullman, Washington.

Oh, Y. H., Han, S. W., and Lee, L. H. (2002). "Effect of boundary element details on the seismic deformation capacity of structural walls." *Earthquake engineering & structural dynamics*, Vol. 31, No. 8, pp. 1583-1602, DOI: 10.1002/eqe.177.

Park, R. (1989). "Evaluation of ductility of structures and structural subassemblages from laboratory testing." *Bull. New Zealand Natl. Soc. Earthquake Eng.*, Vol. 22, No. 3, pp. 155-166.

Thomsen IV, J. H. and Wallace, J. W. (2004). "Displacement-based design of slender reinforced concrete structural walls - experimental verification." *Journal of Structural Engineering*, Vol. 130, No. 4, pp. 618-630, DOI: 10.1061/(ASCE)0733-9445(2004)130:4(618).

Wallace, J. W. and Moehle, J. P. (1992). "Ductility and detailing requirements of bearing wall buildings." *Journal of Structural Engineering*, Vol. 118, No. 6, pp. 1625-1644, DOI: 10.1061/(ASCE)0733-9445(1992)118:6(1625).

Wood, S. L., Wight, J. K., and Moehle, J. P. (1987). *The 1985 Chile earthquake: observations on earthquake-resistant construction in Viña del Mar*, Report UILU-ENG-87-2002, University of Illinois at Urbana-Champaign, Urbana, Illinois.

Yee, A. A. (2001). "Social and environmental benefits of precast concrete technology." *PCI Journal*, Vol. 46, No. 3, pp. 14-19.